Predictive simulations of ionization energies of solvated halide ions with relativistic embedded Equation of Motion Coupled-Cluster Theory

Yassine Bouchafra, Avijit Shee, Florent Réal, Valérie Vallet, André Severo Pereira Gomes

Editors' Suggestion

Predictive Simulations of Ionization Energies of Solvated Halide Ions with Relativistic Embedded Equation of Motion Coupled Cluster Theory

Yassine Bouchafra, Avijit Shee,[†] Florent Réal, Valérie Vallet, and André Severo Pereira Gomes[*]
Université de Lille, CNRS, UMR 8523—PhLAM—Physique des Lasers, Atomes et Molécules, F-59000 Lille, France

(Received 6 November 2018; published 28 December 2018)

A subsystem approach for obtaining electron binding energies in the valence region is presented and applied to the case of halide ions ($X^-, X = \mathrm{F} - \mathrm{At}$) in water. This approach is based on electronic structure calculations combining the relativistic equation-of-motion coupled cluster method for electron detachment and density functional theory via the frozen density embedding approach, using structures from classical molecular dynamics with polarizable force fields for discrete systems (in our study, droplets containing the anion and 50 water molecules). Our results indicate that one can accurately capture both the large solvent effect observed for the halides and the splitting of their ionization signals due to the increasingly large spin-orbit coupling of the $p_{3/2}$-$p_{1/2}$ manifold across the series, at an affordable computational cost. Furthermore, owing to the quantum mechanical treatment of both solute and solvent electron binding energies of semiquantitative quality are also obtained for (bulk) water as by-products of the calculations for the halogens (in droplets).

DOI: 10.1103/PhysRevLett.121.266001

Photoelectron (PE) spectroscopy [1] is a particularly powerful technique (now often complemented by electronic structure calculations) to investigate bound states at the valence or inner regions, either to obtain information on the nature of bonding for species in the gas phase [2–4], in solution [5,6], or at interfaces [7–9] or to follow and identify chemical changes in complex media [10–12]. Such techniques have been extensively used to investigate species such as halogens and halogen-containing species [13–15], which are of great importance in atmospheric processes [16,17] such as photochemical reactions leading to ozone depletion, or aerosol formation [18].

The simplest halogenated systems of relevance are the halides, originating mostly from marine aerosols [19], and understanding how these species interact with water is, apart from its intrinsic interest, of importance for better understanding their effects in the environment. Experimental studies on clusters [20] and bulk [21] aqueous solutions have established that there are very large shifts in the PE spectrum of the halides upon solvation, highlighting strong interactions between the anions and the water solvent. Early theoretical studies determined the halides' electron binding energies (BEs) by employing *ab initio* calculations [22–24] or combining these with classical molecular dynamics simulations with periodic boundary conditions [21]. These studies indicate that not including specific interactions (hydrogen bond, etc.) between the halogens and the solvent water molecules leads to a poor description of the halide BEs [21,25], apart from the fact that quantum-classical approaches cannot yield the electronic structure of the solvent.

Currently the most sophisticated theoretical approaches to obtain PE spectra for the whole system quantum mechanically ("full QM") rely upon density functional theory (DFT) to obtain the ground state for the solvent-solute system (as in Car-Parrinello molecular dynamics (CPMD) [26]), followed by the use of many-body Green's function (MBGF)-based perturbation theories (e.g., *GW* and variants such as G_0W_0 [6,27–31]). MBGF approaches are not without downsides: The first is their high computational cost for fully self-consistent variants, especially if the calculations employ periodic boundary conditions and require large (super)cells. A second, and more serious, issue is the lack of exchange diagrams in self-energy beyond first order. This is particularly a shortcoming in the treatment of molecular systems.

GW-based approaches have been shown to introduce relatively large errors for the calculation of BEs [32,33] compared to reference single-reference coupled cluster [CCSD(T)] or equation-of-motion coupled cluster for electron detachment (EOM-IP-CCSD) [34,35] calculations. Recent benchmarking studies suggest that even lower-scaling, approximate variants to the EOM-CCSD method [36,37] can be competitive in accuracy with *GW* calculations of ionizations and electron affinities, and especially so for G_0W_0 [33].

This Letter presents a full-QM electronic structure approach for obtaining BEs of discrete systems such as water-halide ion ($X^-, X = F - \mathrm{At}$) aggregates, as a cost-effective yet accurate alternative to *GW*-based calculations, by coupling relativistic EOM-IP-CCSD calculations for the halides (since relativistic effects, and in particular

spin-orbit coupling (SOC) [38], on the BEs are increasingly important along the halogen series) and scalar relativistic DFT calculations for the water molecules through the frozen density embedding (FDE) method [39–41].

The key idea of FDE (see Refs. [42–45] for further details and its relationship to other embedding methods) is the partitioning of a system's electron density $n(\boldsymbol{r})$ into a number of fragments [for simplicity two such fragments are considered here, so $n(\boldsymbol{r}) = n_{\mathrm{I}}(\boldsymbol{r}) + n_{\mathrm{II}}(\boldsymbol{r})$] and total energy $E[n(\boldsymbol{r})]$, which can be rewritten as a sum of subsystem energies $(E_i[n_i(\boldsymbol{r})], i = \mathrm{I}, \mathrm{II})$ plus an interaction energy $(E_{(\mathrm{int})})$:

$$E[n] = E_{\mathrm{I}}[n_{\mathrm{I}}] + E_{\mathrm{II}}[n_{\mathrm{II}}] + E_{(\mathrm{int})}[n_{\mathrm{I}}, n_{\mathrm{II}}]. \tag{1}$$

The latter collects the intersubsystem interaction terms,

$$\begin{aligned} E_{(\mathrm{int})}[n_{\mathrm{I}}, n_{\mathrm{II}}] = & \int [n_{\mathrm{I}}(\boldsymbol{r}) v^{\mathrm{II}}_{\mathrm{nuc}}(\boldsymbol{r}) + n_{\mathrm{II}}(\boldsymbol{r}) v^{\mathrm{I}}_{\mathrm{nuc}}(\boldsymbol{r})] d\boldsymbol{r} \\ & + \iint \frac{n_{\mathrm{I}}(\boldsymbol{r}) n_{\mathrm{II}}(\boldsymbol{r}')}{|\boldsymbol{r} - \boldsymbol{r}'|} d\boldsymbol{r} d\boldsymbol{r}' \\ & + E^{\mathrm{nadd}}_{\mathrm{xc}k}[n_{\mathrm{I}}, n_{\mathrm{II}}] + E^{\mathrm{I,II}}_{\mathrm{nuc}}, \end{aligned} \tag{2}$$

where v^{i}_{nuc} is the nuclear potential $(i = \mathrm{I}, \mathrm{II})$, $E^{\mathrm{I,II}}_{\mathrm{nuc}}$ the nuclear repulsion energy between subsystems, and $E^{\mathrm{nadd}}_{\mathrm{xc}k}$ accounts for nonadditive contributions due to the exchange-correlation (xc) and kinetic energy (k) contribution. $E^{\mathrm{nadd}}_{\mathrm{xc}k}$ is defined as

$$\begin{aligned} E^{\mathrm{nadd}}_{\mathrm{xc}k}[n^{\mathrm{I}}, n^{\mathrm{II}}] &= E^{\mathrm{nadd}}_{\mathrm{xc}}[n^{\mathrm{I}}, n^{\mathrm{II}}] + T^{\mathrm{nadd}}_{s}[n^{\mathrm{I}}, n^{\mathrm{II}}] \\ &= E_{\mathrm{xc}}[n^{\mathrm{I}} + n^{\mathrm{II}}] - E_{\mathrm{xc}}[n^{\mathrm{I}}] - E_{\mathrm{xc}}[n^{\mathrm{II}}] \\ &\quad + T_s[n^{\mathrm{I}} + n^{\mathrm{II}}] - T_s[n^{\mathrm{I}}] - T_s[n^{\mathrm{II}}]. \end{aligned} \tag{3}$$

The nonadditive kinetic energy contribution provides a repulsive interaction that offsets the attractive interaction between the nuclear framework of one subsystem and the density of the other [46], which, if not properly matched, can lead to spurious delocalization of the electron density of one subsystem over the region of the other [47] (as seen, for instance, in point-charge or QM–molecular mechanics embedding [48]). For reasons of computational efficiency, the FDE calculations in this Letter employ approximate kinetic energy density functionals [49] which provide good but nevertheless limited accuracy [50] for systems such as those discussed here, which are not covalently bound.

In a purely DFT framework, the density for a subsystem of interest n_{I} is obtained by minimizing the total energy [Eq. (1)] with respect to variations on n_{I} while keeping n_{II} frozen, yielding Kohn-Sham-like equations,

$$[T_{\mathrm{s}}(i) + v_{\mathrm{KS}}[n_{\mathrm{I}}] + v^{\mathrm{I}}_{\mathrm{int}}[n_{\mathrm{I}}, n_{\mathrm{II}}] - \varepsilon_i] \phi^{\mathrm{I}}_i(\boldsymbol{r}) = 0, \tag{4}$$

where $v_{\mathrm{KS}}[n_{\mathrm{I}}]$ and $T_s(i)$ are the usual Kohn-Sham potential and kinetic energy (from $\delta E_{\mathrm{I}}[n_{\mathrm{I}}]/\delta n_{\mathrm{I}}$), and

$$v^{\mathrm{I}}_{\mathrm{int}}(\boldsymbol{r}) = v^{\mathrm{nadd}}_{\mathrm{xc}}(\boldsymbol{r}) + \left.\frac{\delta T^{\mathrm{nadd}}_{s}}{\delta n}\right|_{n_{\mathrm{I}}} + v^{\mathrm{II}}_{\mathrm{nuc}}(\boldsymbol{r}) + \int \frac{n_{\mathrm{II}}(\boldsymbol{r}')}{|\boldsymbol{r} - \boldsymbol{r}'|} d\boldsymbol{r}' \tag{5}$$

is the embedding potential (from $\delta E_{(\mathrm{int})}[n_{\mathrm{I}}, n_{\mathrm{II}}]/\delta n_{\mathrm{I}}$), which describes the interaction between subsystems.

FDE provides a formally exact framework that allows DFT to be replaced by wave function theory (WFT)-based treatments for one [51–54] (WFT-in-DFT) or all subsystems [55] (WFT-in-WFT), with the embedding potential being calculated from Eq. (5) irrespective of the level of electronic structure employed, though using the electron densities from the respective methods. Obtaining electron densities for WFT methods in general and coupled cluster in particular is computationally expensive (the latter requiring the solution of the ground state CC Λ-equations [34]), and it has been found that an approximate scheme—where $v^{\mathrm{I}}_{\mathrm{int}}$ is obtained from preparatory DFT-in-DFT calculations [53,56] and treated as a (local) one-electron operator added to the Fock matrix in the WFT calculations—works very well in practice. This latter prescription is the one followed here.

In the EOM-IP-CCSD method, BEs are obtained from the solution of the eigenvalue equation [35,57]

$$(\bar{H} R^{\mathrm{IP}}_k)_c = \Delta E_k R^{\mathrm{IP}}_k \tag{6}$$

where ΔE_k is the kth ionization energy for the system, $\bar{H} = e^{-T} \hat{H} e^{T}$ is the (CCSD) similarity transformed Hamiltonian [here including $v^{\mathrm{I}}_{\mathrm{int}}(\boldsymbol{r})$] and

$$R^{\mathrm{IP}} = \sum_i r_i \{i\} + \sum_{i>j,a} r^a_{ij} \{a^\dagger j i\} \tag{7}$$

the wave operator that transforms the CC ground state to the electron detachment states.

In the preparatory DFT-in-DFT calculations, the statistical average of model orbital potentials (SAOP) [58] has been used. This potential is constructed to yield Kohn-Sham potentials showing proper atomic shell structure and correct asymptotic behavior, and with it calculations have a computational cost equivalent to Kohn-Sham DFT using generalized gradient approximations. The SAOP orbital energies have been shown to provide BEs that are in very good agreement with coupled cluster calculations [59]. Given the evidence in the literature that Kohn-Sham densities obtained with functionals yielding accurate BEs compare quite well to densities obtained with coupled cluster methods [60,61], a $v^{\mathrm{I}}_{\mathrm{int}}$ obtained with SAOP densities should provide a good approximation to one obtained with coupled cluster densities, with the advantage that one obtains a representation for the PE spectrum of water at no additional cost.

The FDE calculations were performed on structures obtained with classical molecular dynamics (CMD) simulations on water-halide droplets containing 50 water molecules and constraining the halogen to be fixed at the droplet's center of mass, using the POLARIS (MD) code [62–65] and many-body force fields [66] accounting for both polarization effects and the bonding effects within the water molecules (hydrogen bonds), and between the halide and first-hydration shell water units (strong hydrogen bond). From these, after equilibration of the system, were extracted 200 snapshots, which were verified as uncorrelated for the BEs (see the Supplemental Material [67]). A particular feature of the droplet structures for all halogen species, such as that shown in Fig. 1 for a snapshot of solvated I^-, is that the water distribution around the anion is not spherical but elongated due to strong polarization effects that favor disymmetrized structures, with about six to eight water molecules making up the first solvation shell.

The total system was partitioned into two subsystems, the halide (subsystem I) and the 50 water molecules (subsystem II), corresponding to the simplest partition to calculate the halide BEs (referred to as $[X^-@(H_2O)_{50}]$). This choice is supported by benchmark tests (see the Supplemental Material [67]) as well as prior calculations on small halide-water clusters [23], which show that for Cl^-, the valence ionizations are mostly coming from the halide. For F^-, on the other hand, there are important contributions from both the halogen and the waters (with ionization from the latter being lower in energy than from the halide), and because of this a second model was considered in which the nearest eight water molecules are also included in subsystem I [referred to as $([F(H_2O)_8]^-@(H_2O)_{42})$].

The DFT-in-DFT v_{int} were obtained over 200 CMD snapshots with the PYADF scripting environment [69], which used the subsystem DFT implementation in the ADF code [70] and employed the scalar relativistic (SR) zero-order regular approximation (ZORA) Hamiltonian [71] and triple-zeta quality basis sets [72] with two polarization functions for all atoms. The nonadditive kinetic energy and exchange-correlation contributions to v_{int} were calculated with the Lembarki-Chermette (PW91k) [49] and Perdew-Burke-Ernzerhof (PBE) [73] density functionals, respectively. Unless otherwise noted, all SR-ZORA DFT-in-DFT calculations reported use the same computational setup. The embedded EOM-IP-CCSD (EOM) calculations were performed over a subset of 100 CMD snapshots from the originally selected 200 snapshots (see the Supplemental Material [67]) with a development version (revisions e25ea49 and 7c8174a) [57] of the DIRAC electronic structure code [74], using the Dirac-Coulomb (DC) Hamiltonian [38,75] and uncontracted augmented triple-zeta quality [76–78] with two additional diffuse functions for the halogens, and the Dunning aug-cc-pVTZ sets [79] for oxygen and hydrogen. Because of constraints in computational resources for the $([F(H_2O)_8]^-@(H_2O)_{42})$ partition, DFT-in-DFT calculations were performed exclusively using the DC Hamiltonian for F^-. In order to estimate the energies at the complete basis set (CBS) limit calculations with augmented quadruple-zeta basis sets were also performed: for F^- and Cl^-, it was computationally feasible to do so for all snapshots. For the other halides, this was not the case, and estimates for the CBS energies were obtained based on quadruple-zeta calculation on the bare halides. The data set comprising the DFT-in-DFT and CC-in-DFT calculation is available in the Zenodo repository [80].

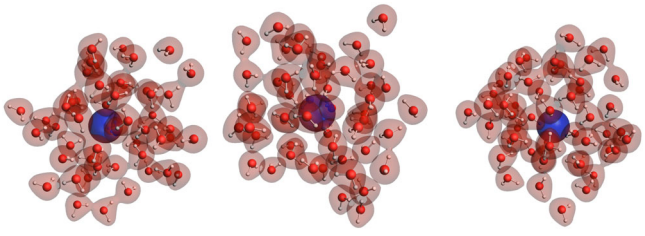

FIG. 1. Views along the (x, y, z) axes for a sample configuration of the CMD simulation for I^-. The (frozen) density for the water subsystem (n_{II}) is superimposed onto the structures [68].

We start by discussing the trends along the series for the BEs over the 100 snapshots, presented in Fig. 2 as histograms plots, with the area under each rectangle being proportional to the number of BEs found at each energy interval. There is very little variation on the BEs of the water subsystems (the yellow and brown rectangles) upon changing the halogen. For the halogens, one finds, first, the displacement of the first ionization energy peak, which in the presence of SOC corresponds to the $^2P_{3/2}$ halogen atom ground electronic states, towards lower energies as the halogen gets heavier. This results in a clear separation between the halogen and water peaks from Br^- onwards. One can also see, as expected from experiments and prior calculations, that irrespective of the treatment of the first solvation shell of F^- (here carried out only with DC SAOP calculations, as explained above), its electron BEs remain entangled with those of the water cluster. Second, the increasing separation between the $^2P_{1/2}$ and $^2P_{3/2}$ components of the halogen ground state is clearly seen, and for I^- the two peaks are clearly distinguishable from those of the water. It is interesting to note, however, that for At^- the SOC effect is so large (with a $^2P_{3/2} - {}^2P_{1/2}$ splitting of $\simeq$3.0 eV) that the $^2P_{1/2}$ peak ends up overlapping with that of water.

Table I summarizes the average BEs for the DFT-in-DFT and CC-in-DFT calculations of Fig. 2 (corresponding to peak maxima), while the experimental results are shown in Table II. By their comparison, one sees that, apart from the F^- case, the EOM results agree rather well with the experimental peak maxima for the halides, with differences of about 0.2 eV for Cl^-, and about 0.1 eV for Br^- and I^-. We attribute this relative improvement along the series to a

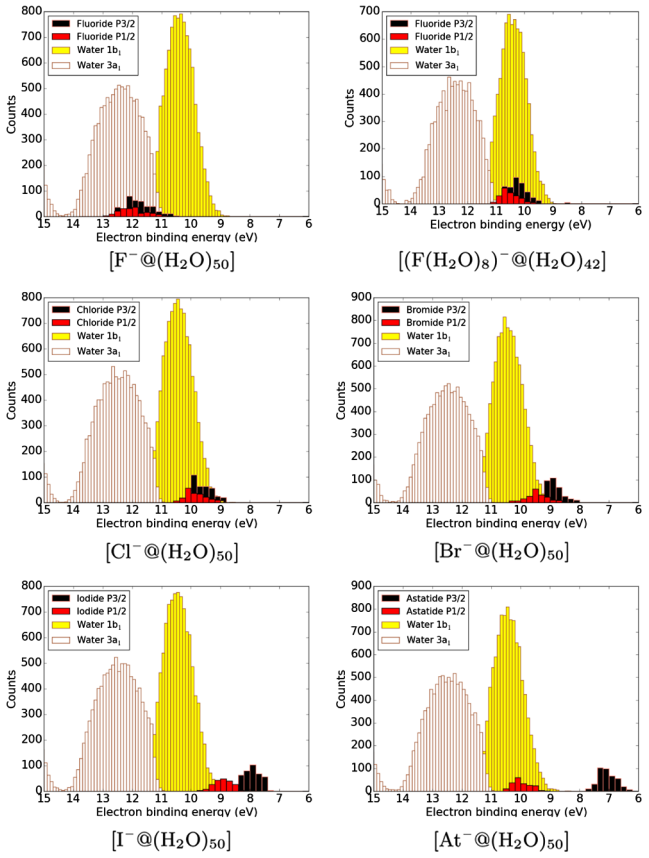

FIG. 2. Electron binding energies spectra for the $[X^-@(H_2O)_{50}]$ systems over the 100 snapshots. Halides BEs obtained with triple-zeta basis sets from DC EOM [except for $([F(H_2O)_8]^-@(H_2O)_{42})$ obtained with DC SAOP] [68].

decrease in entanglement between the halide and the surrounding water molecules as the halide gets heavier [66], which would make our simple embedding model better represent the physical system. For I^-, the only system for which Kurahashi *et al.* [81] provide the spin-orbit splitting of the ^2P state, there is also very good agreement with the experiment for the ionization from the $^2P_{1/2}$ state.

Table I presents results for the halides obtained with triple-zeta base and CBS energy (for F^- and Cl^-) estimates (for Br^- to At^-). A comparison of EOM triple-zeta and CBS results indicates that the latter show a discrete improvement over the former, and in general make our results closer to the experiment. Furthermore, the SAOP results are in rather good agreement with the EOM values, with rather systematic differences on the order of 0.4 eV. This underscored the good performance of SAOP for BEs, especially in view of its modest computational cost, and validates our choice of employing SAOP for the DFT-in-DFT calculations. Additionally, as seen from Table III, SAOP and EOM yield good gas-phase BEs, meaning that the experimental halide BE shifts upon solvation are well reproduced. That said, our embedding model shows what appears to be a systematic underestimation of the water

TABLE I. Average electron binding energies (BE, in eV) for the spin-orbit coupled components of the P states of the hydrated halogens from EOM and SAOP (DC) calculations on the embedded halides with triple-zeta basis sets and the CBS values; and water droplet valence bands from SAOP (SR-ZORA) calculations for the $(H_2O)_{50}$ and $(H_2O)_{42}$ subsystems.

	Halogen				Water	
	$BE_{3/2}$		$BE_{1/2}$		BE_{1b_1}	BE_{3a_1}
Species	EOM	SAOP	EOM	SAOP	SAOP	
	Triple-zeta bases					
F^-	11.8(5)	11.4(5)	12.0(5)	11.5(4)	10.4(5)	12.4(7)
$F(H_2O)_8^-$		10.3(4)		10.5(3)	10.4(5)	12.4(7)
Cl^-	9.7(3)	9.4(4)	9.9(3)	9.5(4)	10.4(5)	12.5(4)
Br^-	9.0(4)	8.7(3)	9.5(4)	9.2(4)	10.4(5)	12.5(4)
I^-	7.9(3)	7.8(3)	8.9(3)	8.6(3)	10.4(5)	12.5(4)
At^-	7.1(3)	7.0(3)	10.0(3)	9.5(3)	10.4(5)	12.5(4)
	CBS (F^-, Cl^-) and CBS[a] (Br^-–At^-)					
F^-	11.9(5)	11.4(5)	12.1(5)	11.5(4)		
$F(H_2O)_8^-$		10.3(4)		10.5(3)		
Cl^-	9.9(3)	9.4(4)	10.1(3)	9.5(4)		
Br^-	9.0(4)	8.7(3)	9.5(4)	9.2(4)		
I^-	8.0(3)	7.8(3)	9.0(3)	8.6(3)		
At^-	7.1(3)	7.0(3)	10.1(3)	9.5(3)		

[a]Estimates from single quadruple-zeta calculations.

spectra, by roughly 1 eV for the b_1 and a_1 peaks. Part of this discrepancy should originate from using SAOP rather than EOM energies (if errors follow those for the halides discussed above, up to 0.4–0.5 eV). We believe that the other major source of errors is the discrete size of the droplets used since the experimental results are for bulk water, and we intend to investigate this issue in a subsequent publication.

For Cl^-, a comparison to prior theoretical results can be made to the G_0W_0 calculations (without SOC) of Gaiduk *et al.* [28], shown in Table IV, for which the most sophisticated calculation using the self-consistent hybrid (sc-hybrid) density functional places the peak position at 9.89 eV. This is higher than the experimental results by a

TABLE II. Experimental electron binding energies (BE, in eV) for the spin-orbit coupled components of the P states of the solvated halide and bulk water valence bands from (a) Kurahashi *et al.* [81], and (b) Winter *et al.* [21].

	Halogen		Water			
	BE_p		BE_{1b_1}		BE_{3a_1}	
Species	(a)	(b)	(a)	(b)	(a)	(b)
F^-	9.8					
Cl^-	9.5(2)	9.60(7)				
Br^-	9.00(7)	8.80(6)				
		8.1(1)				
I^-	8.03(6)[a]	7.7(2)[a]	11.31(4)	11.16(4)	13.78(7)[b]	13.50(10)
	8.96(7)[c]	8.8(2)[c]				

[a]$\Omega = 3/2$.
[b]Average value of the $3a_1$ H and $3a_1$ L bands.
[c]$\Omega = 1/2$.

TABLE III. Gas-phase electron binding energies (BE, in eV) for the halides (DC) and the water molecule (SR-ZORA, PBE optimized geometry).

		SAOP		EOM		
Species		Triple-zeta	CBS	Triple-zeta	CBS	Expt.
F^-	$BE_{3/2}$	3.16	3.16	3.32	3.45	3.40 [82,83]
Cl^-	$BE_{3/2}$	3.41	3.41	3.59	3.77	3.62 [84,85]
Br^-	$BE_{3/2}$	3.23	3.23	3.40	3.48	3.37 [86,87]
I^-	$BE_{3/2}$	3.02	3.02	3.12	3.19	3.06 [88]
At^-	$BE_{3/2}$	2.48	2.48	2.41	2.55	2.40[a] [89]
H_2O	BE_{1b_1}	12.33				12.62 [90]

[a]CCSD(T).

little over 0.3 eV. It is also higher than the EOM calculations, even if it is compared to our ^2P term value of 9.76 eV. The G_0W_0–sc-hybrid calculations show very good agreement with experiment for the water peaks, though a comparison to our results would be somewhat biased since the G_0W_0 ones are made for a bulk liquid, and ours are not. It is important to note that the G_0W_0 results do not show very good agreement with the experimental BEs if less sophisticated functionals such as PBE and PBE0 are used—in fact, the DC SAOP results are of slightly better quality than those.

Another relevant comparison is with the electron propagator calculations of Dolgounitcheva *et al.* [23], performed for microsolvated clusters of F^- and Cl^- and including the effect of outer solvation shells via the PCM. For Cl^-, the propagator results agree well with each other but are nevertheless 0.7–1 eV higher than the experiment, whereas our results are not more than 0.2 eV higher. For the first ionization of F^- to which there are significant contributions from Dyson orbitals on F, the propagator results are closer to each other but again quite far from the experiment. If part of the discrepancy comes from differences in treatment of electron correlation between the propagators and EOM (or SAOP) and basis set effects (bases smaller than ours were used), the most significant contribution should be due to the explicit inclusion of the outer solvation shells in our calculations. The importance of this effect is seen in the P3 calculations of Canuto *et al.* [91], which, when considering outer-shell effects via point-charge embedding, recover nearly 2.5 eV with respect to the microsolvated ion, showing an agreement to experiment similar to SAOP.

TABLE IV. Selected theoretical electron binding energies (BE, in eV) from the literatures for solvated F^- and Cl^- using the G_0W_0 [28] approach, and the Outer-Valence Greens Function (OVGF), Partial third order (P3) and renormalized Partial third order (P3+) propagator approaches combined with PCM (polarizable continuum model) [23] or explicit solvation (PC, point-charge embedding) [91].

Method	Cl^-	F^-
G_0W_0-PBE [28]	8.76	
G_0W_0-PBE0 [28]	9.43	
G_0W_0-RSH [28]	9.86	
G_0W_0–sc-hybrid [28]	9.89	
OVGF-PCM [23]	10.53	10.70
P3-PCM [23]	10.32	12.21
P3 + -PCM [23]	10.29	12.02
P3-6H_2O [91]	6.95	
P3-6H_2O + 60H_2O(PC) [91]	9.41	

In conclusion, our results show that FDE is a viable method for obtaining quantitatively accurate electron binding energies (and with that simulate PE spectra) in the valence region for species in solution. For systems not undergoing chemical changes, the combination of CC-in-DFT calculations with CMD simulations with polarizable force fields can yield results which rival much more sophisticated simulation approaches, but at a much smaller computational cost (the embedded EOM calculations take about a day per snapshot on four cores for At^-, the most expensive calculations). In this sense, the SAOP model potential appears to be a rather interesting alternative to more computationally expensive functionals by itself or, eventually, being combined with many-body treatments based on the *GW* method. Finally, our work was based on droplet simulations, which can be interesting to investigate systems made up by a relatively small amount of water molecules, though monitoring droplet size effects on such properties and their convergence towards the bulk requires further investigation. The FDE calculations are, however, completely agnostic to the nature of the procedure employed to obtain the structures, and they can be equally applied to snapshots from standard (or FDE-based [92]) CPMD calculations (whenever DFT-based interaction potentials are sufficiently accurate [93]) or static band-structure FDE calculations [94] that naturally describe long-range interactions in extended systems.

We acknowledge support from the Labex CaPPA (Chemical and Physical Properties of the Atmosphere, Contract No. ANR-11-LABX-0005-01), CPER CLIMIBIO (European Regional Development Fund, Hauts de France council, French Ministry of Higher Education and Research), the CNRS Institute of Physics (PICS Grant No. 6386), and French national supercomputing facilities (Grant No. DARI A0030801859).

*Corresponding author.
andre.gomes@univ-lille.fr
†Present address: Department of Chemistry, University of Michigan, 930 North University, Ann Arbor, Michigan 48109-1055, USA.

[1] J. L. Bahr, Contemp. Phys. **14**, 329 (1973).
[2] P. D. Dau, J. Su, H.-T. Liu, D.-L. Huang, J. Li, and L.-S. Wang, J. Chem. Phys. **137**, 064315 (2012).

[3] W.-L. Li, J. Su, T. Jian, G. V. Lopez, H.-S. Hu, G.-J. Cao, J. Li, and L.-S. Wang, J. Chem. Phys. **140**, 094306 (2014).
[4] J. Su, P. D. Dau, H.-T. Liu, D.-L. Huang, F. Wei, W. H. E. Schwarz, J. Li, and L.-S. Wang, J. Chem. Phys. **142**, 134308 (2015).
[5] R. Seidel, B. Winter, and S. E. Bradforth, Annu. Rev. Phys. Chem. **67**, 283 (2016).
[6] T. A. Pham, M. Govoni, R. Seidel, S. E. Bradforth, E. Schwegler, and G. Galli, Sci. Adv. **3**, e1603210 (2017).
[7] P. S. Bagus, E. S. Ilton, and C. J. Nelin, Surf. Sci. Rep. **68**, 273 (2013).
[8] L. Trotochaud, A. R. Head, O. Karslıoğlu, L. Kyhl, and H. Bluhm, J. Phys. Condens. Matter **29**, 053002 (2017).
[9] A. Knop-Gericke, V. Pfeifer, J.-J. Velasco-Velez, T. Jones, R. Arrigo, M. Hävecker, and R. Schlögl, J. Electron Spectrosc. Relat. Phenom. **221**, 10 (2017).
[10] X. Kong, A. Waldner, F. Orlando, L. Artiglia, T. Huthwelker, M. Ammann, and T. Bartels-Rausch, J. Phys. Chem. Lett. **8**, 4757 (2017).
[11] T. Bartels-Rausch, F. Orlando, X. Kong, L. Artiglia, and M. Ammann, ACS Earth Space Chem. **1**, 572 (2017).
[12] A. A. Raheem, M. Wilke, M. Borgwardt, N. Engel, S. I. Bokarev, G. Grell, S. G. Aziz, O. Kühn, I. Y. Kiyan, C. Merschjann, and E. F. Aziz, J. Biomol. Struct. Dyn. **4**, 044031 (2017).
[13] B. P. Tsal, T. Baer, A. S. Werner, and S. F. Lin, J. Phys. Chem. **79**, 570 (1975).
[14] M. K. Gilles, M. L. Polak, and W. C. Lineberger, J. Chem. Phys. **96**, 8012 (1992).
[15] A. F. Lago, J. P. Kercher, A. Bödi, B. Sztáray, B. Miller, D. Wurzelmann, and T. Baer, J. Phys. Chem. A **109**, 1802 (2005).
[16] W. R. Simpson, S. S. Brown, A. Saiz-Lopez, J. A. Thornton, and R. von Glasow, Chem. Rev. **115**, 4035 (2015).
[17] A. Saiz-Lopez, J. M. C. Plane, A. R. Baker, L. J. Carpenter, R. von Glasow, J. C. Gómez Martín, G. McFiggans, and R. W. Saunders, Chem. Rev. **112**, 1773 (2012).
[18] J. C. Gómez Martín, O. Gálvez, M. T. Baeza-Romero, T. Ingham, J. M. C. Plane, and M. A. Blitz, Phys. Chem. Chem. Phys. **15**, 15612 (2013).
[19] L. J. Carpenter and P. D. Nightingale, Chem. Rev. **115**, 4015 (2015).
[20] G. Markovich, S. Pollack, R. Giniger, and O. Cheshnovsky, J. Chem. Phys. **101**, 9344 (1994).
[21] B. Winter, R. Weber, I. V. Hertel, M. Faubel, P. Jungwirth, E. C. Brown, and S. E. Bradforth, J. Am. Chem. Soc. **127**, 7203 (2005).
[22] A. K. Pathak, T. Mukherjee, and D. K. Maity, Chem. Phys. Lett. **454**, 17 (2008).
[23] O. Dolgounitcheva, V. G. Zakrzewski, and J. V. Ortiz, Int. J. Quantum Chem. **112**, 3840 (2012).
[24] Z. He, G. Feng, B. Yang, L. Yang, C.-W. Liu, H.-G. Xu, X.-L. Xu, W.-J. Zheng, and Y. Q. Gao, J. Chem. Phys. **148**, 222839 (2018).
[25] M. P. Coons and J. M. Herbert, J. Chem. Phys. **148**, 222834 (2018).
[26] J. Hutter, Comput. Mol. Sci. **2**, 604 (2012).
[27] C. Zhang, T. A. Pham, F. Gygi, and G. Galli, J. Chem. Phys. **138**, 181102 (2013).
[28] A. P. Gaiduk, M. Govoni, R. Seidel, J. H. Skone, B. Winter, and G. Galli, J. Am. Chem. Soc. **138**, 6912 (2016).
[29] A. P. Gaiduk and G. Galli, J. Phys. Chem. Lett. **8**, 1496 (2017).
[30] A. P. Gaiduk, J. Gustafson, F. Gygi, and G. Galli, J. Phys. Chem. Lett. **9**, 3068 (2018).
[31] A. P. Gaiduk, T. A. Pham, M. Govoni, F. Paesani, and G. Galli, Nat. Commun. **9**, 247 (2018).
[32] X. Blase, P. Boulanger, F. Bruneval, M. Fernandez-Serra, and I. Duchemin, J. Chem. Phys. **144**, 034109 (2016); **145**, 169901 (2016).
[33] M. F. Lange and T. C. Berkelbach, J. Chem. Theory Comput. **14**, 4224 (2018).
[34] R. J. Bartlett and M. Musiał, Rev. Mod. Phys. **79**, 291 (2007).
[35] R. J. Bartlett, Comput. Mol. Sci. **2**, 126 (2012).
[36] J. J. Goings, M. Caricato, M. J. Frisch, and X. Li, J. Chem. Phys. **141**, 164116 (2014).
[37] A. K. Dutta, N. Vaval, and S. Pal, Int. J. Quantum Chem. **118**, e25594 (2018).
[38] T. Saue, Chem. Phys. Chem. **12**, 3077 (2011).
[39] P. Cortona, Phys. Rev. B **44**, 8454 (1991).
[40] P. Cortona, Phys. Rev. B **46**, 2008 (1992).
[41] T. A. Wesołowski and A. Warshel, J. Phys. Chem. **97**, 8050 (1993).
[42] A. S. P. Gomes and C. R. Jacob, Annu. Rep. Prog. Chem., Sect. C: Phys. Chem. **108**, 222 (2012).
[43] C. R. Jacob and J. Neugebauer, Comput. Mol. Sci. **4**, 325 (2014).
[44] T. A. Wesołowski, S. Shedge, and X. Zhou, Chem. Rev. **115**, 5891 (2015).
[45] Q. Sun and G. K.-L. Chan, Acc. Chem. Res. **49**, 2705 (2016).
[46] O. Roncero, M. P. de Lara-Castells, P. Villarreal, F. Flores, J. Ortega, M. Paniagua, and A. Aguado, J. Chem. Phys. **129**, 184104 (2008).
[47] C. R. Jacob, S. M. Beyhan, and L. Visscher, J. Chem. Phys. **126**, 234116 (2007).
[48] P. Reinholdt, J. Kongsted, and J. M. H. Olsen, J. Phys. Chem. Lett. **8**, 5949 (2017).
[49] A. Lembarki and H. Chermette, Phys. Rev. A **50**, 5328 (1994).
[50] A. W. Götz, S. M. Beyhan, and L. Visscher, J. Chem. Theory Comput. **5**, 3161 (2009).
[51] N. Govind, Y. A. Wang, and E. A. Carter, J. Chem. Phys. **110**, 7677 (1999).
[52] T. A. Wesołowski, Phys. Rev. A **77**, 012504 (2008).
[53] A. S. P. Gomes, C. R. Jacob, and L. Visscher, Phys. Chem. Chem. Phys. **10**, 5353 (2008).
[54] S. Höfener, A. S. P. Gomes, and L. Visscher, J. Chem. Phys. **136**, 044104 (2012).
[55] S. Höfener and L. Visscher, J. Chem. Phys. **137**, 204120 (2012).
[56] S. Höfener, A. S. P. Gomes, and L. Visscher, J. Chem. Phys. **139**, 104106 (2013).
[57] A. Shee, T. Saue, L. Visscher, and A. S. P. Gomes, J. Chem. Phys. **149**, 174113 (2018).
[58] O. V. Gritsenko, P. R. T. Schipper, and E. J. Baerends, Chem. Phys. Lett. **302**, 199 (1999).
[59] P. Tecmer, A. S. P. Gomes, U. Ekström, and L. Visscher, Phys. Chem. Chem. Phys. **13**, 6249 (2011).

[60] I. Grabowski, A. M. Teale, S. Śmiga, and R. J. Bartlett, J. Chem. Phys. **135**, 114111 (2011).
[61] D. S. Ranasinghe, A. Perera, and R. J. Bartlett, J. Chem. Phys. **147**, 204103 (2017).
[62] M. Masella, Mol. Phys. **104**, 415 (2006).
[63] M. Masella, D. Borgis, and P. Cuniasse, J. Comput. Chem. **32**, 2664 (2011).
[64] M. Masella, D. Borgis, and P. Cuniasse, J. Comput. Chem. **34**, 1112 (2013).
[65] J. P. Coles and M. Masella, J. Chem. Phys. **142**, 024109 (2015).
[66] F. Réal, A. S. P. Gomes, Y. O. Guerrero Martínez, T. Ayed, N. Galland, M. Masella, and V. Vallet, J. Chem. Phys. **144**, 124513 (2016).
[67] See Supplemental Material at http://link.aps.org/supplemental/10.1103/PhysRevLett.121.266001 for atomic calculations, benchmarks calculations with FDE models, time-correlations of properties, basis set convergence tests.
[68] Y. Bouchafra, A. Shee, F. Real, V. Vallet, and A. S. P. Gomes, http://dx.doi.org/10.5281/zenodo.1477103.
[69] C. R. Jacob, S. M. Beyhan, R. E. Bulo, A. S. P. Gomes, A. W. Götz, K. Kiewisch, J. Sikkema, and L. Visscher, J. Comput. Chem. **32**, 2328 (2011).
[70] C. R. Jacob, J. Neugebauer, and L. Visscher, J. Comput. Chem. **29**, 1011 (2008).
[71] E. van Lenthe, E. J. Baerends, and J. G. Snijders, J. Chem. Phys. **99**, 4597 (1993).
[72] E. van Lenthe and E. J. Baerends, J. Comput. Chem. **24**, 1142 (2003).
[73] J. P. Perdew, K. Burke, and M. Ernzerhof, Phys. Rev. Lett. **77**, 3865 (1996); **78**, 1396 (1997).
[74] L. Visscher *et al.* (DIRAC Collaboration), computer code DIRAC, 2017 release, 2017, http://www.diracprogram.org.
[75] L. Visscher, Theor. Chem. Acc. **98**, 68 (1997).
[76] K. G. Dyall, Theor. Chem. Acc. **108**, 335 (2002).
[77] K. G. Dyall, Theor. Chem. Acc. **115**, 441 (2006).
[78] K. G. Dyall, Theor. Chem. Acc. **135**, 128 (2016).
[79] R. A. Kendall, T. H. Dunning, Jr., and R. J. Harrison, J. Chem. Phys. **96**, 6796 (1992).
[80] Y. Bouchafra, A. Shee, F. Real, V. Vallet, and A. S. P. Gomes, http://dx.doi.org/10.5281/zenodo.1477004.
[81] N. Kurahashi, S. Karashima, Y. Tang, T. Horio, B. Abulimiti, Y.-I. Suzuki, Y. Ogi, M. Oura, and T. Suzuki, J. Chem. Phys. **140**, 174506 (2014).
[82] H.-P. Popp, Z. Naturforsch. **22A**, 254 (1967).
[83] R. Milstein and R. S. Berry, J. Chem. Phys. **55**, 4146 (1971).
[84] G. Mück and H.-P. Popp, Z. Naturforsch. **23A**, 1213 (1968).
[85] I. S. McDermid and C. R. Webster, J. Phys. (Paris), Colloq. **44**, C7-461 (1983).
[86] R. S. Berry and C. W. Reimann, J. Chem. Phys. **38**, 1540 (1963).
[87] H. Frank, M. Neiger, and H.-P. Popp, Z. Naturforsch. **25A**, 1617 (1970).
[88] C. R. Webster, I. S. McDermid, and C. T. Rettner, J. Chem. Phys. **78**, 646 (1983).
[89] A. Borschevsky, L. F. Pašteka, V. Pershina, E. Eliav, and U. Kaldor, Phys. Rev. A **91**, 020501 (2015).
[90] J. E. Reutt, L. S. Wang, Y. T. Lee, and D. A. Shirley, J. Chem. Phys. **85**, 6928 (1986).
[91] S. Canuto, K. Coutinho, B. J. C. Cabral, V. G. Zakrzewski, and J. V. Ortiz, J. Chem. Phys. **132**, 214507 (2010).
[92] A. Genova, D. Ceresoli, A. Krishtal, O. Andreussi, R. A. DiStasio, Jr., and M. Pavanello, Int. J. Quantum Chem. **117**, e25401 (2017).
[93] M. J. Gillan, D. Alfè, and A. Michaelides, J. Chem. Phys. **144**, 130901 (2016).
[94] J. Tölle, A. S. P. Gomes, P. Ramos, and M. Pavanello, Int. J. Quantum Chem. **119**, e25801 (2018).